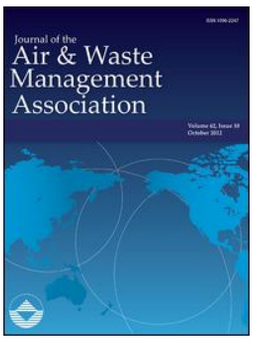

Taylor & Francis
Taylor & Francis Group

Journal of the Air & Waste Management Association

ISSN: 1096-2247 (Print) 2162-2906 (Online) Journal homepage: http://www.tandfonline.com/loi/uawm20

Estimating Maximum Concentrations for Open Path Monitoring Along a Fixed Beam Path

Michael G. Yost , Ram A. Hashmonay , Yi Zhou , Robert Spear , DooYong Park & Steven Levine

To cite this article: Michael G. Yost , Ram A. Hashmonay , Yi Zhou , Robert Spear , DooYong Park & Steven Levine (1999) Estimating Maximum Concentrations for Open Path Monitoring Along a Fixed Beam Path, Journal of the Air & Waste Management Association, 49:4, 424-433, DOI: 10.1080/10473289.1999.10463820

To link to this article: https://doi.org/10.1080/10473289.1999.10463820

TECHNICAL PAPER

ISSN 1047-3289 *J. Air & Waste Manage. Assoc.* **49**:424-433

Estimating Maximum Concentrations for Open Path Monitoring Along a Fixed Beam Path

Michael G. Yost and Ram A. Hashmonay
School of Public Health and Community Medicine, University of Washington, Seattle, Washington

Yi Zhou and Robert Spear
School of Public Health, University of California, Berkeley, California

DooYong Park and Steven Levine
School of Public Health, University of Michigan, Ann Arbor, Michigan

ABSTRACT

Researchers have applied open path optical sensing techniques to a variety of workplace and environmental monitoring problems. Usually these data are reported in terms of a path-average (or path-integrated) concentration. When assessing potential human exposures along a beam path, this path-average value is not always informative, since concentrations along the path can vary substantially from the beam average. The focus of this research is to arrive at a method for estimating the upper-bound in contaminant concentrations over a fixed open beam path. The approach taken here uses a statistical model to estimate an upper-bound concentration based on a combination of the path-average and a measure of the spatial variability computed from point samples along the beam path. Results of computer simulations and experimental testing in a controlled ventilation chamber indicate that the model produced conservative estimates for the maximum concentration along the beam path. This approach may have many applications for open path monitoring in workplaces or wherever maximum concentrations are a concern.

IMPLICATIONS

Many environmental regulations and emergency decisions are based on maximum allowable air concentrations, whether at a fence line, near an area source, or at an indoor worksite. In principle, open path monitoring continuously samples all points along a beam path and can better identify any potential emissions compared to a few point monitors. However, open path sampling produces path-integrated data, which can be interpreted as the spatial average over points arrayed in a line. Using only the simplest reduction of the data as a path-average makes interpretation of the results in terms of a maximum concentration problematic. This paper presents a statistical framework for combining point and open path sample data to estimate the maximum concentration anywhere along the beam path. Experimental validation indicates that this approach should provide good estimates of maximum concentration from open path monitoring.

INTRODUCTION

The first studies to report optical remote sensing of emissions appeared in the literature almost two decades ago. Initial experiments using open path infrared beams to monitor the atmosphere are summarized in the work of Stevens and Herget.[1] These remote sensing systems offered a glimpse of a revolutionary new technology where monitoring systems could "look across" an environmental site, locate air contaminants, and quantify the concentrations.[2] Although early instruments appeared promising, they were so large that they occupied a 40-ft trailer.[3] Early work applied this technique to monitoring stacks and other fixed location sources; later research began investigating open path monitoring for vehicle emissions and mobile sources.[4]

Fourier transform infrared (FTIR) spectroscopy for workplace sampling was introduced in the 1980s.[5] Early research used a gas cell instrument and collected samples with conventional pumps but demonstrated the practical utility of FTIR analysis methods for sampling industrial chemicals.[6,7] Later research conducted the first open path FTIR (OP-FTIR) field studies for workplace sampling of volatile organic solvents and chamber studies to validate the analytical accuracy of OP-FTIR methods in comparison to conventional flame ionization point sampling.[8–10] In recent years, research has provided important new OP-FTIR methods for workplace sampling including a new technique for generating background spectra,[11] the use of time series analysis to detect changes from normal operation and

the first field testing of fixed beam monitoring for process control,[12] and the first experimental testing of computed tomography methods for reconstructing gaseous contaminant distributions indoors.[13–17] This research has significantly advanced OP-FTIR technology from a laboratory curiosity to a valuable, practical tool for workplace and environmental monitoring.

Significance for Exposure Monitoring

Exposure characterization remains a central feature of regulatory and industrial hygiene decisionmaking; it guides decisions about regulatory compliance and the allocation of resources for intervention. Development of OP-FTIR technology for exposure monitoring is important for two reasons: (1) convenient routine exposure assessment is crucial to decisionmaking and (2) the dearth of reasonable alternative sampling methods for labile, volatile, or polar compounds alone or when they occur as components in complex mixtures.

Characterization of exposures for a variety of situations remains difficult. As an example, consider the situation for monitoring exposures in workplaces. A recent American Conference of Government Industrial Hygienists Threshold Limit Values (ACGIH-TLV) booklet lists about 160 compounds with Short-Term Exposure (STE) limits or ceiling values, which account for more than 20% of all the listings. A ceiling limit is a maximum value never to be exceeded, while STE represents an average concentration over any 15-min period. Sampling for these compounds, which have short-term or ceiling limits, is often problematic because of the difficulty of selecting a representative peak exposure sampling interval and the high variability of short-term point samples. Some compounds, particularly reactive species, polar species, or complex mixtures, can be difficult to sample with conventional methods. In these situations, OP-FTIR sampling provides the advantage of (1) measuring agents in situ without the need for pumps, tubes, or other sampling apparatus that might introduce sampling losses; (2) rapid, continuous measurements with sample intervals as fast as a few seconds; (3) the ability to resolve individual components in complex mixtures; and (4) the ability to qualitatively identify unknown chemical species or intermediate reaction products.

An OP-FTIR spectrometer measures the amount of infrared light absorbed at specific wavelengths by molecules along a beam path, providing an estimate of the quantity of contaminants inside the volume of the beam path. All molecules of a particular contaminant in the beam path volume contribute to the measured absorbance, so the instrument measures the integrated absorbance from molecules over the total path length, usually expressed as ppm-meters. Dividing the measured path-integrated concentration by the total path length gives the path-average concentration.

However, when assessing potential exposures along a beam path, this calculated path-averaged concentration is not always informative since concentrations at points along the path can vary substantially from the path-average. In general, the path-average will differ from an individual's average exposure. In fact, the path-average concentration equals the personal exposure only in well mixed situations. A fixed beam instrument can make no distinction, for example, between 1 ppm of a contaminant well mixed throughout a 100-m beam path and 100 ppm of contaminant all contained only within 1 m of an otherwise uncontaminated 100-m beam path. The two different scenarios would yield the same path-integrated measurement of 100 ppm-meters. Because the path length is the same, both situations also would have the same calculated path-average concentration (1 ppm). Yet for human exposure assessment or regulatory decisions the distinction between these two situations can be vital.

The objective of this work was to determine if practical limits on personal exposure along a beam path can be constructed from beam data under various mixing conditions. We describe how the beam path-average can give useful estimates of the highest likely exposures using an appropriate statistical model and a measure of the spatial variability in contaminant concentrations along the beam path. The solution developed here involves two important insights: (1) the maximum likely concentration depends upon the degree of spatial variability in concentrations along the beam path, and (2) one can make a statistical prediction of the upper-bound based upon a beam path-averaged measurement and a measure of the spatial variation in concentration derived from concurrent point samples taken at fixed locations along the beam. These two ideas are explored further below in a conceptual model describing the degree of mixing along the beam path.

The Gamma Model

The underlying model for predicting maximum exposures along a beam path is depicted in Figure 1. Consider a beam path with total volume, V, divided into N = 10 equal sized control segments V_i (i = 1,2,.....N). Each control segment (V_i) is assumed to contain a homogeneous concentration C_i and is of some fixed breathing zone dimensions (e.g., a cylinder of 30-cm [1 ft] long with the circular cross section of the beam [typically 20–30-cm diameter]. Alternatively, for a well-collimated beam of constant diameter one could define a control segment length, L_i, and N would represent the number of these segments in the total beam path length L. The maximum personal exposure is just the maximum concentration, or upper-bound concentration (C_{max} = Maximum{C_i}), among these N control segments of

the beam path. This concentration maximum in turn depends on how the contaminant molecules are dispersed along the beam path.

A mixing factor, gamma (γ), can be used to relate the maximum concentration along the beam (C_{max}) to the beam average concentration, C_b. Gamma is bounded within a range of [L_i/L, 1] by two extreme cases, which characterize the degree of departure from the beam path-averaged concentration in Figure 1. In the "best case" corresponding to perfect mixing along the beam path, C_{max}= C_b =10 ppm, and γ equals 1/N; in the "worst case," all the contaminant molecules reside only in a single control segment, C_{max}= (L/ L_i) * C_b =100 ppm and γ=1. In practice, γ will lie between these two extremes with its value depending upon the spatial inhomogeneity in concentration. From the preceding we can generalize this concept to any number of control segments along the beam path by the equation

$$C_{max} = \gamma \cdot \frac{L}{L_i} \cdot C_b = \gamma \cdot N \cdot C_b \qquad (1)$$

where L = total beam path length, L_i = control segment length, N = the number of control segments, C_b = beam path-average concentration, C_{max} = upper-bound concentration associated with control segment L_i, and γ = a mixing factor relating the maximum concentration to the path average.

Various factors contribute to γ or the mixing along a path. The spatial variability in contaminant levels for a given exposure environment depends upon both source characteristics and dispersion or ventilation conditions. An indoor exposure environment at steady state with fixed source locations or a fairly constant air exchange rate would have a characteristic γ value and appear nearly time-stationary. Combining this γ value along with real-time C_b measurements would provide an estimate of the upper-bound concentration over a beam path and the probable approximate location.

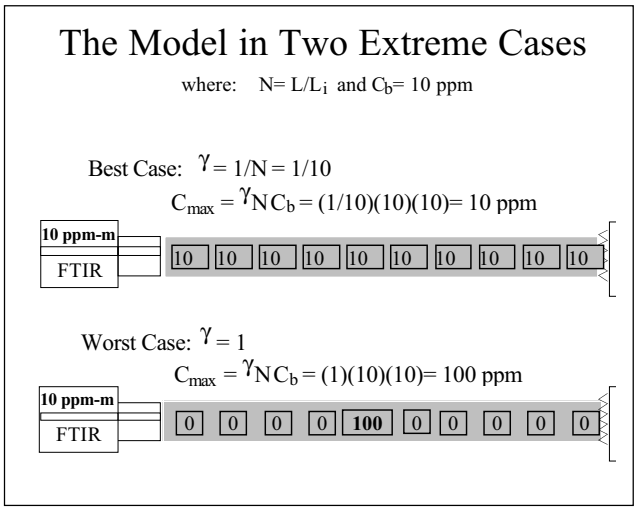

Figure 1. Schematic of the gamma model under two extreme situations, corresponding to completely homogeneous and inhomogenous concentration distributions along a beam path.

The critical feature for applying this model to OP-FTIR monitoring is to arrive at a practical method for estimating γ over a given beam path. The approach taken here is to obtain a combination of beam path and point sample data to experimentally estimate γ. For example, this could take the form of a "calibration experiment," deploying a series of sampling pumps and bags along the beam path to collect the point sample data. To avoid further complexities introduced by different averaging times, we will describe here only situations where the beam and point samples are collected over the same time period.

Estimating Gamma

A direct method of determining γ would use N point samplers uniformly spaced along the beam path to measure concentrations in all N control segments. Simultaneously an average beam concentration C_b is measured with an OP-FTIR system along with the maximum concentration Max{C_i} observed from the array of point samplers. Then the sample estimate (indicated by a hat symbol, ^) for γ is

$$\hat{\gamma} = \frac{\text{Max}\{C_i\}}{(N \cdot C_b)} \qquad (2)$$

There are several weaknesses associated with this estimate for γ. One weakness arises from the assumption of a homogeneous concentration in each control segment L_i. A limited number of discrete point samplers may not necessarily capture the real maximum concentration, resulting in an underestimation of the true γ. Second, the precision of the γ estimate may be poor, due to the potentially high variability of Max{Ci}. Finally, for moderately long beam paths of, say, >30 m, this approach requires an unrealistic number of point samples.

An alternative procedure for estimating γ can be based on the relationship between γ and some measure of the spatial variability of concentrations along a beam path. As a measure of this spatial variability, we propose a spatial coefficient of variation, CV_s, defined as

$$CV_s = \frac{1}{C_b}\sqrt{\frac{\sum_{i=1}^{k}(C_i - C_b)^2}{k}} \qquad (3)$$

where C_b is the beam path-average concentration measured by the OP-FTIR, and C_i represents the individual point concentrations measured at the ith discrete location along the beam path. Note that C_b, the beam average, appears here in

the definition of CV_s instead of the Average$\{C_i\}$. Although the two averages are theoretically equal given the assumption of a homogeneous concentration in each L_i, they are not necessarily equal in practice, especially when a more limited number of point samplers are used. We use C_b in computing spatial variability because it always represents the true average value of contaminant concentration over all possible locations along the beam path.

Since CV_s describes the spatial variability or mixing conditions along the beam, presumably CV_s will be a reasonably good predictor of γ and some functional relationship exists between the two quantities (i.e., $\gamma = \{CV_s\}$). Knowing the functional relationship between these variables, one could predict γ from a sample estimate of CV_s. This approach avoids the weaknesses of the previous direct method based on measuring $Max\{C_i\}$ for two reasons. First, CV_s gives a summary statistic derived from all sampled locations. Consequently it has less variability compared to that of the single maximum value, thereby yielding a γ estimate with improved stability. Second, a sample estimate of CV_s may be less sensitive to decreasing the number of point samples compared to estimating $Max\{C_i\}$. This latter advantage has practical importance because a useful estimate of γ may be obtained with relatively few point samples.

To explore this concept further, we undertook computer simulation experiments to determine the relationship between γ and CV_s. The results of these simulation experiments, presented below, indicate the existence of a quasi-linear relationship between CV_s and γ. More importantly, the simulations show that this relationship can be bounded in all cases by a line.

Simulation Tests

Computer simulation experiments were used to study the relationship between CV_s and γ. A random concentration value was assigned to each of N control segments for a fixed beam path length, creating one computer realization of a mixing condition. CV_s and γ were then calculated from the N concentrations and stored. A wide range of spatial variations in concentrations along a beam path were created by repeating the simulation many times with different lengths and also using different random simulation algorithms.

Note that the value of CV_s or γ does not depend on the functional form of the spatial distribution (e.g., Gaussian, triangle, or log-normal) used for concentrations along the path. This is easily demonstrated for a given realization of $\{C_i\}$ distributed among N compartments, because γ, C_b, and CV_s remain invariant regardless of how the N compartments are rearranged, sorted, or ordered. This adds to the robustness of the estimation method since it involves no assumptions about the spatial distribution of the contaminant.

Simulation Results

Figure 2 shows the relationship between CV_s and γ for a realization of N = 10 control segments resulting from 200 computer simulation runs. From many such simulations, we postulated the existence of a near-linear relationship between CV_s and γ, with the maximum value bounded by a line given by

$$\hat{\gamma} = \frac{1}{N} + \frac{(1-\frac{1}{N})}{\sqrt{(N-1)}} \cdot CV_s \qquad (4)$$

and

$$\hat{C}_{max} = \hat{\gamma} \cdot N \cdot C_b = C_b + \frac{(N-1)}{\sqrt{(N-1)}} \cdot C_b \cdot CV_S \qquad (5)$$

The line represented by eq 4 (also shown in Figure 2) gives an upper-bound line for all realizations of γ and CV_s. The parameters for the equation of this line are determined by the two extremes discussed earlier as the well mixed case and the single compartment or worst case conditions: for the well mixed case, $CV_s = 0$ and $\gamma = L_i/L = 1/N$; for the worst case, $\gamma = 1$ and $CV_s = CV_{max} = \sqrt{(N-1)}$. The derivation for CV_{max} used to obtain the upper limit is given in the Appendix.

The relationship between CV_s and γ remains consistent under various simulation algorithms. After trying several approaches, we settled on the following method, which efficiently generated a wide range of γ and CV_s values. This algorithm, used extensively to generate the simulation results reported here, included two steps. First, randomly select K control segments ($K \leq N$) to have nonzero concentrations. Second, assign a random concentration uniformly distributed in the range of (0, C) independently to each of

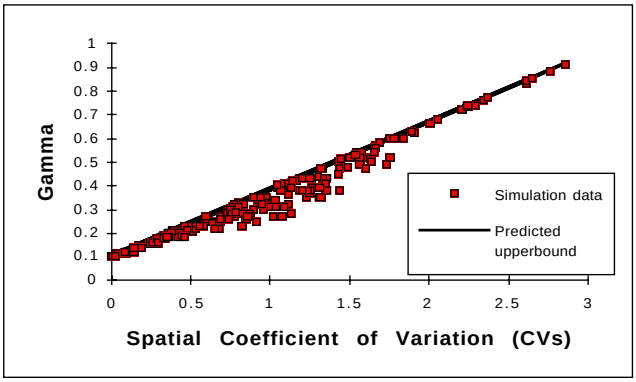

Figure 2. Scatterplot of computer simulation results for the gamma model along a three-meter (10-ft) beam path. The points represent the outcome of each random realization of a beam concentration distribution, while the line represents the upper-bound γ value predicted from the linear model in eq 4.

the K control segments. Then calculate CV_s and γ and store the values. The actual magnitude of C for the simulation algorithm was arbitrary and can be viewed as the maximum possible concentration of a contaminant occurring along the beam path. Regardless of the algorithm used, we found that eq 4 provided a conservative upper-bound γ value for a particular value of CV_s. Conversely, given a sample estimate of CV_s it should be possible to use eq 5 to generate an estimate of the upper-bound concentration along a beam path.

Experimental Verification of the Simulation Results

Based on theoretical and simulation results, we next conducted a series of chamber experiments with SF_6 as a tracer gas to test the gamma model. The experiments were conducted in a controlled ventilation chamber that has been described previously. [9] As a practical experimental matter, we had to define a reasonable minimum control segment so that all possible control segments along the path could be sampled in our studies. We assumed that the spacing between samplers, and therefore the length of a control segment for a person's breathing zone, is about 30 cm (1 ft) along a 20-cm diameter beam path. Our use of one point sampler per beam segment is required only in the context of our experimental validation tests, which used eq 2 to find γ. In general, it is not a constraint when applying the gamma model in a field situation where only a sample estimate of CV_s is desired.

Conventional point samples were drawn for 15-min intervals using personal sampling pumps and sampling bags; these bag samples were subsequently analyzed using a Brüel and Kjær (B&K) 1302 photoacoustic gas analyzer. The B&K photoacoustic analyzer was calibrated using 1 ppm and 50 ppm ±2% span gas references. An MDA OP-FTIR system simultaneously collected path-averaged data during the 15-min sampling period. The OP-FTIR data were subsequently analyzed using a 10 ppm-meter library reference spectrum of sulfur hexafluoride and classical least squares quantification with LabCalc software.

A series of eight experiments in the test chamber used a 3-m (10-ft) beam path and 10 Tedlar bag samplers spaced at equal intervals along the beam path to measure concentrations in each control segment. We produced various mixing conditions by placing two tracer sources at different distances relative to the beam path or by adjusting the source strength and location.

Figure 3 presents the observed and predicted results for γ. These results agreed very well with the simulations, and the predicted maximum value for γ from eq 4. In these experiments, γ increases almost linearly with an increasing value of CV_s. Further, the γ value predicted by eq 4 shows a close correspondence to the observed values of γ from the experiments but in every case remained conservative. We attempted to create a wide range of CV_s values in the experiments, which have a theoretical upper-bound of $CV_s = 3$ as described in the Appendix (based on N = 10 control segments along the path). But, apparently, values of CV_s that are much beyond 2 are difficult to obtain in our experimental setting, and the highest observed value was only approximately 80% of the expected range.

Figure 4 presents a comparison of the maximum values predicted by eq 5 for these experiments and the observed maximum concentration along the path. Of course, given the correspondence in γ values in Figure 3, the upper-bound also agrees closely with the observations. Still, Figure 4 illustrates that, in every case, the model predicts a conservative upper-bound, and this predicted maximum shows fairly precise agreement with the observed maximum measured with the closely spaced point samplers.

Chamber Experiments Simulating Exposure Conditions

A second series of 20 experiments was undertaken to provide a somewhat more realistic test of field conditions. In these experiments, only a few point samplers were used along a beam path to obtain a sample estimate of CV_s. The upper-bound concentration predicted by the gamma model from this sample CV_s and the beam average was then compared to the STE observed for an individual walking along the beam path. Further details of the experimental setup are described elsewhere,[12] so only a brief account appears here related to the setup shown in Figure 5.

In this experimental series, we equally spaced seven bag samplers along a 7.3-m beam path. An acetone vapor generator provided the tracer gas. Two 1-cm ceramic ball diffusers were used as point emission sources. One diffuser was located in the inlet plenum and was well mixed

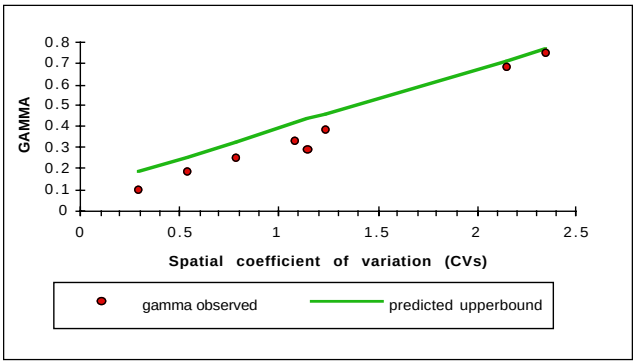

Figure 3. Scatterplot of experimental results for the gamma model from chamber studies of a 3-m (10-ft) beam path. The points represent the outcome of 10 experiments where beam concentration distributions were measured simultaneously with point samplers in each control segment and with an OP-FTIR measuring the entire beam path. The line represents the upper-bound γ value predicted from the linear model in eq 4. In all cases the linear model gives conservative (higher) γ values.

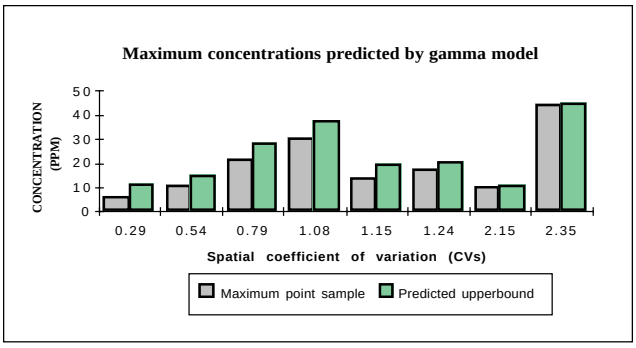

Figure 4. Plot of observed and predicted maximum concentrations from experimental chamber studies of a 3-m (10-ft) beam path. The bars represent the outcome of 10 experiments with concentrations measured simultaneously with point samplers in each control segment and an OP-FTIR covering the entire beam path. Predicted maximum values were generated based on eq 5. In all cases the linear gamma model gives conservative (higher) values.

with the incoming air to create a general room background. The second point source was located inside the chamber upwind of the beam path to simulate a local high concentration plume. We produced various spatial tracer gas distribution conditions in our chamber by changing the ventilation in the room, the location of the leak source, and emission rates from the two sources. Different ventilation conditions were obtained by using additional mixing fans (see Figure 5) and changing air exchange rates in the chamber to give room time constants of 1.5 or 5 min. During the experiments, the background source in the inlet plenum was switched on and off at 1-min intervals by a computer-controlled valve according to a binary random sequence to simulate normal source variability.

Each experiment lasted approximately 45 min. Bag samples were collected along the beam path for consecutive 15-min intervals during a test using sample pumps drawing 0.2 L/min into 10-L Tedlar bags. At the end of a session all bags were analyzed with a flame ionization detector (FID), calibrated for acetone as described below. During a session, FTIR interferograms were collected at two scans per second (2 cm^{-1} spectral resolution), co-averaged over 30-sec intervals, and stored for later analysis. The FTIR data analysis used CLS quantification with 30-sec values averaged into 15-min averages corresponding to the same time intervals as the bag samples.

As part of the experiments, a person wearing a real-time sampler walked along the beam path. In about 1-min intervals the subject moved to one of 4 randomly assigned locations (A, B, C, D) representing four of the 24 possible control segments along the beam path. A sampling tube connected to the FID provided real-time

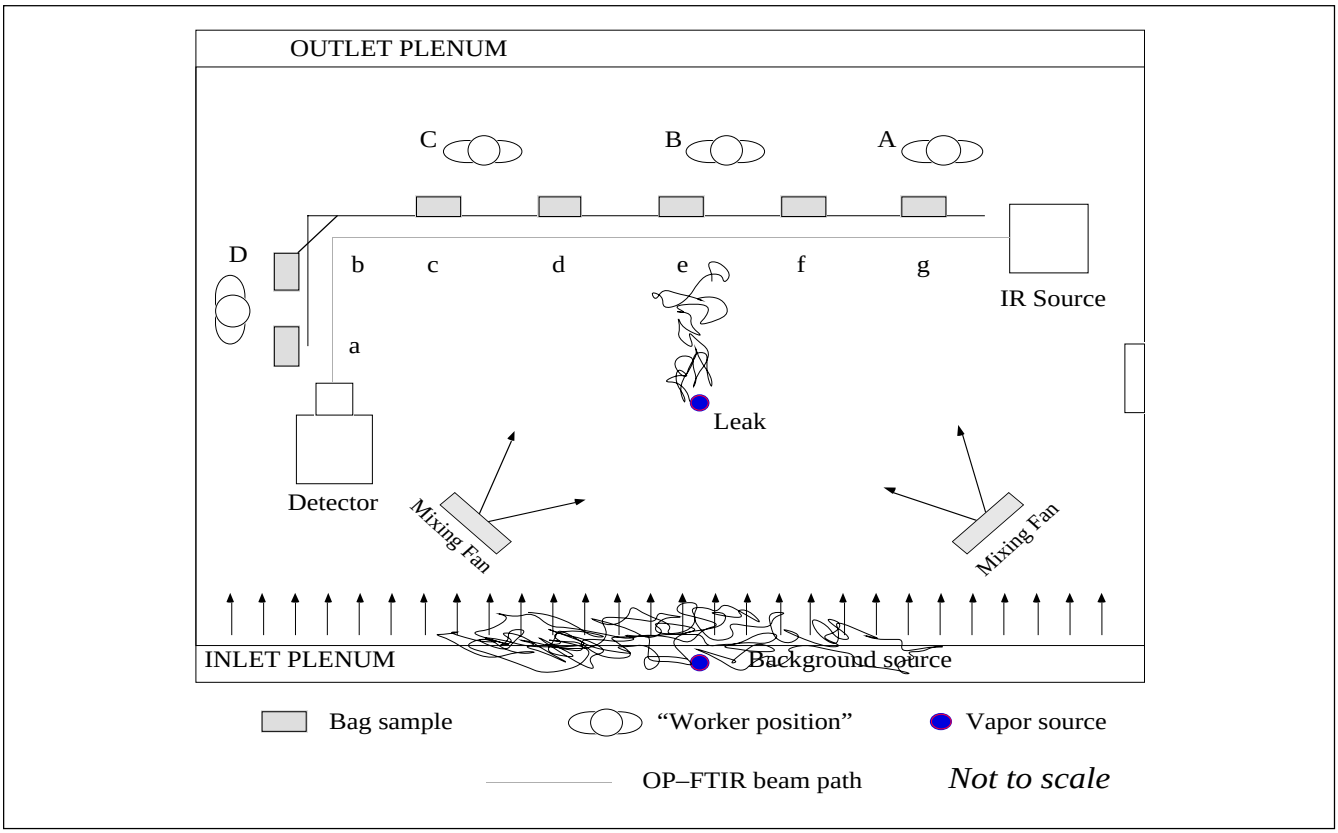

Figure 5. Diagram of the experimental setup for chamber studies of personal exposures along a 7.3-m beam path. Locations a–g correspond to the point samplers uniformly spaced along the path. Locations A–D correspond to one realization of four subject positions randomly assigned during an experimental session. Note that subject locations do not necessarily correspond to point sampler locations.

measurements of the acetone concentration in the breathing zone; the response time of the FID (0 to 90%) was about 10 sec. The FID electronic signal was sent to a data logger (1 sample/sec) and averaged over 15-min intervals to create a STE personal sample value during the session. The FID was calibrated at 50 and 200 ppm ±2% with span gas from cylinders (Scott Specialty Gas).

Each 15-min interval was taken as one realization of a gamma model that generated (1) averages from the FTIR, (2) point samples for estimating γ along the beam path, and (3) a 15-min STE personal exposure. The results of these experiments comparing the $\hat{C}_{max}$ predicted by the gamma model and the personal exposures appear in Figure 6. These experiments achieved a somewhat wider range of CV_s values but still well below the theoretical maximum of 4.8 In all cases, the gamma model with sample estimates of CV_s predicted a conservative upper-bound concentration compared to the actual 15-min STE from the personal sampler.

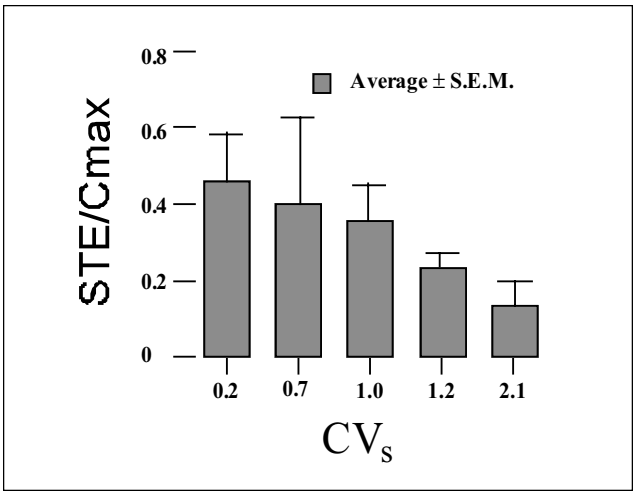

Figure 6. The plot shows the ratio of personal 15-min short-term exposure limit (STE) concentrations divided by the maximum concentrations predicted with eq 5. This comparison is given for several values of CV_s. Data bars represent the average and standard error of mean of three or four trials per CV_s condition from the experimental chamber studies of a person standing at random locations along a 7.3-m (24-ft) beam path. Concentrations were measured simultaneously with a real-time monitor in the breathing zone, an OP-FTIR measuring the entire path, and seven point samplers uniformly spaced along the beam path. In all cases, the gamma model gives conservative (higher) estimated maximum values compared to a personal STE value over the same time interval, with a trend toward more conservative predictions at higher values of CVs.

DISCUSSION

Often in practice the number of point samples will be much less than the number of control segments, so these only yield an estimate of the true CV_s. For example, our tests only sampled one-third of the control segments in the 7.3-m path. When sampling to estimate γ, the underlying statistical distribution of concentration values becomes important in evaluating the number of samples required to achieve some desired precision. Using more point samples should produce a better γ estimate, but because we lack information on the statistical distribution of point samples, it remains somewhat unclear how many samples to take to get a stable estimate. For example, if $\{C_i\}$ has a normal distribution, then one could use a chi-square distribution to construct a confidence interval around CV_s for a particular sample size. Yet at least in extreme cases, the distribution probably is not normal, approaching a binary condition (e.g., either high or low concentration) in the worst case. A similar problem arises in how to arrange point samples along the beam path; ideally, randomly sampling compartments along a beam path achieves an unbiased estimate. However, when only a few points will be measured, uniformly spaced sampling seems a reasonable strategy since random assignment may sometimes "clump" samples together along the path. Further evaluation of sampling schemes could be done by computer simulation studies, provided some reasonable distribution assumptions can be applied.

Examining the equations for the gamma model provides additional insight into the statistical framework. We know that the limiting case where γ = 1 represents a binary spatial concentration distribution. Let us define $\hat{p}$ = 1/N as the minimum proportion of the beam path containing high contaminant levels and $\hat{q}$ = (1 - $\hat{p}$) as the proportion containing low (or possibly zero) concentrations. With some manipulation, one can rewrite eq 4 in the form

$$\hat{\gamma} = \hat{p} + \hat{q} \cdot \frac{\hat{CV}_S}{CV_{Max}} = \hat{p} + \hat{q} \cdot \frac{\sqrt{\frac{1}{k}\sum_{i=1}^{k}(C_i - C_b)^2}}{N \cdot C_b \cdot \sqrt{\hat{p} \cdot \hat{q}}} \quad (6)$$

The above equation suggests that the γ estimate expressed in eq 4 comes from the limiting binary concentration distribution. This gamma estimate represents a weighted linear combination of the proportion of the beam containing high and low concentrations. The weighting factor is the ratio of the observed variability from the k point samples (where k ≤ N) over the variability of the limiting binary case. The gamma estimate in eq 6 selects this binary concentration distribution so it has the same mean and variance as that observed from the beam and point samples. Thus, another interpretation to the gamma model is that it represents *any* observed spatial concentration distribution in terms of a limiting binary case: a single control segment having a high concentration of C_{max} and the remaining beam having a lower concentration of

$$C_{low} = (1-\gamma) \cdot C_b \cdot N/(N-1) \quad (7)$$

We also note that eq 7 suggests an alternative way of estimating γ, based on obtaining a sample estimate of C_{low} rather than based on CV_s. For example, we could choose to estimate C_{low} by taking the average concentration of all the point samples with values below the beam average, that is $\hat{C}_{low}$ = Average{ $C_i \mid C_i \le C_b$ }. In extreme situations where γ really is close to 1, this method of estimating γ may be more efficient since it is quite likely that a point sample will come from a control segment representing the lower bound concentration.

To investigate the effects of sampling on γ estimates, we conducted a type of bootstrap analysis on the data described earlier in connection with Figures 3 and 4. We performed 200 trials each having a random sample without replacement of size k = 2, 3, 4, 6 from the 10 points measured along a beam path. We estimated gamma with eqs 6 and 7 (calculating $\hat{C}_{low}$ as suggested above) for each trial and compared the sample estimates to the true γ values based on knowing all points along the path. The results are shown in Table 1, expressed as the percentage error in the sample estimate. With a large sample size (k = 6), the CV_s equation always produced unbiased estimates with average error near zero. The CV_s equation produced relatively unbiased estimates even for small sample sizes with $\gamma \le 0.5$, but shows a tendency to underestimate γ, which grows quite severe in some cases ($\gamma \ge 0.7$). As anticipated, for large γ values ($\gamma \ge 0.7$) eq 7 appears to perform better, but at intermediate γ values, it has a large, although conservative, bias. Both methods of estimating γ can have considerable variability when based on a small number of samples. Again as expected, for moderate γ values eq 6 seems to have lower variability, whereas at extreme values eq 7 performs better.

The above analysis supports and amplifies the observations made earlier in the discussion: The performance of sample γ estimates largely depends on the underlying statistical distribution of $\{C_i\}$. The gamma model is the limiting binary case regardless of the sample distribution. However, the sample distribution can strongly influence the parameter estimators (i.e., $\hat{CV}_S$ or $\hat{C}_{low}$) for the gamma model. We presented two approaches for estimating γ, but further research could examine parameter estimators that are robust and efficient for minimal sample size.

The gamma model was intended primarily for workplace monitoring, where it could be applied either to short-term exposure (e.g., STE values) or long-term (e.g., full-shift TWA) monitoring. For example, different γ values could be derived to estimate 15-min upper-bounds versus 8-hr upper limits, which may have different variability. In either case the beam and point samples should be averaged over the same time interval. Applying short-term measurements to estimate long-term maxima could prove difficult due to the autocorrelation and typically higher variability found in short-term data and the potential for nonrepresentative sampling conditions.

We purposely restricted our experiments to situations having concurrent point and beam samples and to estimating the upper-bound during the sampling interval. This rather narrow set of conditions was selected because it provided a statistically rigorous test of the gamma model. In actual practice we would like to limit the need for costly and difficult point sampling. Perhaps a more typical application would involve taking point and beam samples at one time, estimating γ, and then applying the γ value in subsequent time intervals with new beam data to estimate an upper-bound. This approach of using a sort of "calibration experiment" involves the important additional assumption of a time-stationary mixing condition along the beam path. In many indoor workplaces with mechanical ventilation, this assumption may be justified, but in outdoor settings it may prove tenuous. In outdoor situations it may be necessary to incorporate meteorological data or other indicators of atmospheric mixing conditions rather than attempt to continuously gather both beam and point samples. Thus, outdoors a more practical approach may be to combine mixing factors derived from dispersion modeling with the gamma model to update the upper-bound estimates. This would be a likely avenue for future research.

Table 1. Percent error in γ estimates based on bootstrap analysis of experimental data.

	Estimated by eq 6				Estimated by eq 7 [c]			
	Number of point samples				Number of point samples			
True γ [a]	2	3	4	6	2	3	4	6
0.2	0 ± 17 [b]	0 ± 14	0 ± 10	1 ± 6	35 ± 58	28 ± 44	27 ± 34	27 ± 22
0.3	-4 ± 20	-1 ± 16	0 ± 13	0 ± 9	68 ± 53	69 ± 36	68 ± 31	72 ± 20
0.4	-7 ± 28	-6 ± 23	-3 ± 18	-1 ± 13	89 ± 29	91 ± 22	88 ± 22	90 ± 15
0.5	-9 ± 35	0 ± 31	-5 ± 25	0 ± 18	79 ± 12	79 ± 11	79 ± 8	80 ± 5
0.7	-22 ± 40	-12 ± 43	-16 ± 43	-4 ± 33	17 ± 22	14 ± 19	14 ± 13	15 ± 10
0.8	-32 ± 35	-20 ± 40	-13 ± 41	-5 ± 35	6 ± 29	2 ± 22	5 ± 18	4 ± 13

[a] Expected γ value if all points in the beam path are sampled. [b] All values are average % error ± standard deviation from 200 random trials. [c] C_{low} estimated by the average of all point samples ≤ beam path-average.

Working with our collaborators in industry, we had an opportunity to discuss the type of practical applications this work might address. One such application that sparked interest concerned the use of OP-FTIR monitoring to determine respiratory protection requirements for workers entering normally unoccupied areas for maintenance or other episodic operations. This problem also applies to waste sites, which may require workers to wear a self-contained breathing apparatus (SCBA) because of the uncertainty about exposures rather than because of any measured exposure hazard. In both applications, OP-FTIR measurements may provide useful information regarding the appropriate respirator requirements.

Alternatively, we can view this work in the context of the NIOSH respiratory protection decision logic.[18] The decision logic specifies three key requirements for when to allow the use of air-purifying respirators: (1) knowledge of the identity of all air contaminants, (2) knowledge of the air concentration of air contaminants, and (3) whether conditions immediately dangerous to life or health (conditions IDLH) may occur. If the above are undetermined, the default selection of personal protective equipment reverts to a supplied air respirator or SCBA; if the identity and concentration of the contaminants are known, adequate warning properties exist (e.g., odor or irritating properties) at levels below the permissible exposure limits and where conditions IDLH cannot occur, air-purifying respirators or working without respirators may be permitted.

Our results indicate that beam path monitoring coupled with some knowledge of γ may provide the information needed to address the above requirements. Therefore, using OP-FTIR to estimate maximum concentrations could have applications to decisions regarding personnel protective equipment in workplaces or at waste sites and in adjacent fence line areas.[19,20] Also, OP-FTIR technology can effectively monitor mixtures, labile, or polar compounds as well as more common volatile organics, which other monitoring systems target. With the availability of OP-FTIR systems, the appropriate level of respiratory protection may be chosen based on real data rather than on uninformed default assumptions.

The practical implications of this work are that the gamma model provides a statistical framework for predicting maximum personal exposures along a fixed beam path. In the worst case, available without any knowledge of point samples, the concentration is no higher than the beam concentration multiplied by the number of control segments of some minimum defined size. Typically, this worst case estimate is extremely conservative. By using point samplers along the beam path, one can measure spatial variability or some other parameter and refine the upper-bound estimate along the path. Importantly, it appears from these experiments that the gamma model also offers reasonable bounds on STEs measured along the beam path.

The need for using point samplers comes about because the beam path was fixed in these studies. However, with a scanning beam system it becomes possible to segment the OP-FTIR beam path to gather information on the spatial distribution of contaminants along the path.[21] If this information can be used to estimate γ, then a scanning beam system may require little or no point sampling information to estimate maximum exposures, a hypothesis we propose to explore in future research.

ACKNOWLEDGMENT

Partial financial support for this work was provided by the National Institute for Occupational Safety and Health (NIOSH), grant R01-OH-02666; the Consortium for Risk Evaluation with Stakeholder Participation (CRESP), US Department of Energy Cooperative Agreement #DE-FCO1-95EW55084; the Seattle Foundation Grant #632144; and the ALCOA Science Foundation.

REFERENCES

1. Stevens, R.K.; Herget, W.F., Eds. *Analytical Methods Applied to Air Pollution Measurements*; Ann Arbor Science: Ann Arbor, MI, 1974.
2. McClenny, W.A.; Herget, W.F.; Stevens, R.K. A Comparative Review of Open-Path Spectroscopic Absorption Methods for Ambient Air Pollutants. In *Analytical Methods Applied to Air Pollution Measurements;* Stevens, R.K.; Herget, W.F., Eds.; 1990; Chapter 6.
3. Herget W.F.; Brasher, J.D. "Remote optical sensing of emissions," *Applied Optics* **1979**, *18,* 3044–8.
4. Herget, W.F.; Staab, J.; Klinerberg, H.; Reidel, W.J. Progress in the Prototype Development of the New Multicomponent Exhaust Gas Sampling and Analyzing System. Presented at the Society of Automotive Engineers, Detroit, MI, Feb 1984; Paper #840470.
5. Herget, W.F.; Levine, S.P. "Fourier transform infrared (FTIR) spectroscopy for monitoring semiconductor process gas emissions," *Appl. Ind. Hygiene* **1986**, *1,* 110–112.
6. Ying, L.S.; Levine, S.P. "FTIR least-squares methods for the quantitative analysis of multi-component mixtures of airborne vapors of IH concern," *Anal. Chem.* **1989**, *61,* 677–683.
7. Ying, L.S.; Levine, S.P.; Strang, C.R.; Herget, W.F. "FTIR spectroscopy for monitoring airborne gases and vapors of IH concern," *Am. Ind. Hyg. Assoc. J.* **1989**, *30,* 354–359.
8. Xiao, H.K.; Levine, S.P.; Puskar, M.A.; Nowak, J.; Spear, R.C. "Analysis of organic vapors in the workplace by remote sensing FTIR," *Am. Ind. Hyg. Assoc. J.* **1993**, *54,* 545–556.
9. Yost, M.G.; Spear, R.C.; Xiao, H.K.; Levine, S.P. "Comparative testing of a remote sensing optical system with area samplers in a controlled ventilation chamber," *Am. Ind. Hyg. Assoc. J.* **1992**, *53,* 611–616.
10. Todd, L.; Ramachandran, G. "Evaluation of an infrared open-path spectrometer using an exposure chamber and a calibration cell," *Am. Ind. Hyg. Assoc. J.* **1995**, *56,* 151–157.
11. Xiao, H.K.; Levine, S.P. "Differential method for open path-FTIR," *Anal. Chem.* **1993**, *65,* 2262–2269.
12. Malachowski, M. S.; Levine, S. P.; Herrin, G.; Spear, R. C.; Yost, M.G.; Yi Zhou "Workplace and environmental air contaminant concentrations measured by open path Fourier transform infrared spectroscopy: a statistical process control technique to detect changes from normal operating conditions," *J. Air & Waste Manage. Assoc.* **1994**, *44,* 673–682.
13. Yost, M.G.; Drescher, A.C.; Yi Zhou; Saisan, P.; Simonds, M.A.; Nazaroff, W.W.; Levine, S.P.; Gadgil, A.J. "Imaging indoor tracer-gas concentrations with computed tomography: experimental results with a remote sensing FTIR system," *Am. Ind. Hyg. Assoc. J.* **1994**, *55,* 395–402.
14. Drescher, A.C.; Nazaroff, W.W.; Yost, M.G.; Park, D.Y.; Levine, S.P.; Gadgil, A.J. Measurement of Tracer Gas Distributions Using an Open Path FTIR System Coupled With Computed Tomography. In *Proceedings of the International Symposium on Optical Remote Sensing for Environmental and Process Monitoring*; Air & Waste Management Association: Pittsburgh, PA, 1994; VIP-37/SPIE 2365, 128.

15. Park, D.Y.; Yost, M.G.; Levine, S.P. "Evaluation of virtual source beam configurations for rapid tomographic reconstruction of gas and vapor concentrations in workplaces," *J. Air & Waste Manage. Assoc.* **1997**, *47,* 582–591.
16. Drescher, A.C.; Park, D.Y.; Yost, M.G.; Gadgil, A.J.; Levine, S.P.; Nazaroff, W.W. "Indoor measurement of stationary and time-dependent tracer gas concentration profiles using open path FTIR remote sensing and SBFM computed tomography," *Atmos. Env.* **1997**, *31,* 727–740.
17. Hashmonay, R.A.; Yost, M.G.; Wu, C.F. Computed Tomography of Air Pollutants Using Radial Scanning Path-Integrated Optical Remote Sensing. *Atmos. Env.* **1999**, *33*, 267-274.
18. Bollinger, N.J.; Shultz, R.H. *NIOSH Guide to Industrial Respiratory Protection*; U.S. Department of Health and Human Services: Cincinnati, OH, 1987; pp 87–116.
19. Levine, S.P.; Turpin, R.D.; Gochfeld, M. "Protecting personnel at hazardous waste sites: current issues," *App. Occup. Environ. Hyg.* **1991**, *6,* 1007–1014.
20. Lolgin, E.; Poziomek, E. "Advances in field screening methods for hazardous waste site investigations," *Am. Environ. Lab.* **1990**, 18–24.
21. Hashmonay, R.A.; Yost, M.G.; Mamane, Y.; Benayahu, Y. Emission Rate Apportionment from Fugitive Sources Using Open-Path FTIR and Mathematical Inversion. *Atmos. Environ.* **1999**, 33, 735-743.

APPENDIX

Derivation of CV_{max}

$$\sum_{i=1}^{N} C_i = N \cdot C_b$$

Given:

$$Var\{C_i\} = \frac{1}{N}\sum_{i=1}^{N}(C_i - C_b)^2$$

$$Var\{C_i\} = \frac{1}{N}\left(\sum_{i=1}^{N} C_i^2 - 2 \cdot C_b \cdot \sum_{i=1}^{N} C_i + \sum_{i=1}^{N} C_b^2\right)$$

$$Var\{C_i\} = \frac{1}{N}\left(\sum_{i=1}^{N} C_i^2 - N \cdot C_b^2\right)$$

$$Var\{C_i\} = \frac{1}{N}\sum_{i=1}^{N} C_i^2 - C_b^2$$

$$Var_{\max}\{C_i\} = Max\left\{\frac{1}{N}\sum_{i=1}^{N} C_i^2\right\} - C_b^2$$

So, since

$$\sum_{i=1}^{N} C_i^2 < \left(\sum_{i=1}^{N} C_i\right)^2$$

then,

$$Max\left\{\sum_{i=1}^{N} C_i^2\right\} = N^2 \cdot C_b^2 = C_c^2$$

So maximum variance occurs in the worst case where

$C_c = N * C_b$ and all other cells have zero.

$$Var_{\max}\{C_i\} = \frac{1}{N} \cdot (N \cdot C_b)^2 - C_b^2 = C_b^2 (N-1)$$

So,

$$CV^2_{\max} = \frac{Var_{\max}}{C_b^2} = N - 1$$

$$CV_{\max} = \sqrt{(N-1)}$$

About the Authors

Michael G. Yost (airion@u.washington.edu) is an Associate Professor and Ram A. Hashmonay is a Research Associate in the Department of Environmental Health in the School of Public Health and Community Medicine at the University of Washington. Both can be reached at Box 357234, School of Public Health and Community Medicine, Department of Environmental Health, University of Washington, Seattle, WA 98195-7243. Yi Zhou is a Ph.D. candidate and Robert Spear is a Professor in the Department of Environmental Health Sciences, School of Public Health, University of California at Berkeley, Berkeley, CA 94720. DooYong Park is an Assistant Professor in the Department of Environmental Safety Engineering, Hansung University, 389 Samsun-dong 2 Ga, Sung Guk-ku, Seoul 136-792, Korea. Steven Levine is a Professor in the Department of Environmental and Industrial Health, School of Public Health, University of Michigan, Ann Arbor, MI 48109